

**Studies on Langmuir monolayers and
Langmuir-Blodgett films of mesogenic
and organometallic molecules**

by

Raj Kumar Gupta

**Thesis submitted to the
Jawaharlal Nehru University
for the award of the degree of
Doctor of Philosophy**

June 2005



***Raman Research Institute
Bangalore 560 080
India***

CERTIFICATE

This is to certify that the thesis entitled **Studies on Langmuir monolayers and Langmuir-Blodgett films of mesogenic and organometallic molecules** submitted by Raj Kumar Gupta for the award of the degree of DOCTOR OF PHILOSOPHY of Jawaharlal Nehru University is his original work. This has not been published or submitted to any other University for award of other degree or diploma.

Prof. N. Kumar

(Center Chairperson)

Director

Raman Research Institute

Bangalore 560 080 - INDIA

Prof. Kattera A. Suresh

(Thesis Supervisor)

DECLARATION

I hereby declare that this thesis is composed independently by me at the Raman Research Institute, Bangalore, under the supervision of Prof. Kattera A. Suresh. The subject matter presented in this thesis has not previously formed the basis for the award of any degree, diploma, membership, associateship, fellowship or any other similar title of any University or Institution.

(Prof. Kattera A. Suresh)

Liquid Crystal Laboratory

Raman Research Institute

Bangalore 560 080 - INDIA

(Raj Kumar Gupta)

Contents

1	Introduction	1
1.1	Experimental Techniques	3
1.1.1	Monolayer and multilayer at air-water interface	3
1.1.1.1	Surface manometry	3
1.1.1.2	Epifluorescence microscope	7
1.1.1.3	Brewster angle microscope	8
1.1.2	Monolayer and multilayer at air-solid interface	9
1.1.2.1	Scanning probe microscopes	12
1.1.2.2	Grazing angle reflection absorption infrared spectroscopy	14
1.2	Two-dimensional phases in Langmuir monolayer	15
1.3	Mixed monolayers	18
1.4	Molecules forming Langmuir monolayer and Langmuir-Blodgett films . . .	18
2	Studies on the monolayer of cholesteric acid	23
2.1	Introduction	23
2.2	Experimental	23
2.3	Results	24
2.3.1	Langmuir monolayer of cholesteric acid on ion-free water	24
2.3.2	Metal complexes of cholesteric acid monolayer	31
2.4	Discussion	37
2.5	Conclusions	42

3	Mixed monolayers of cholesteric acid and lipid molecules	46
3.1	Introduction	46
3.2	Experimental	47
3.3	Results and Discussion	47
3.3.1	Mixed monolayer of cholesteric acid and cholesterol	47
3.3.2	Mixed monolayer of cholesteric acid and stearic acid	57
3.3.3	Mixed monolayer of cholesteric acid and DPPC	63
3.4	Conclusions	71
4	Mixed monolayer of cholesterol and thiocholesterol	75
4.1	Introduction	75
4.2	Experimental	76
4.3	Results	76
4.4	Discussion	80
4.5	Conclusions	86
5	AFM studies on Langmuir-Blodgett films of cholesterol	89
5.1	Introduction	89
5.2	Experimental	90
5.3	Results and Discussion	91
5.4	Conclusions	102
6	Ordering of cholesterol molecules on graphite: STM and computer simulation studies	106
6.1	Introduction	106
6.2	Experimental	106
6.3	Results and Discussion	108
6.4	Simulations	110
6.5	Conclusions	116

7	Monolayer of disk-like mesogenic molecules	118
7.1	Introduction	118
7.2	Experimental	118
7.3	Results	120
7.4	Discussion	123
8	Studies on monolayer of functionalized gold particles	129
8.1	Introduction	129
8.2	Experimental	130
8.3	Results	131
8.4	Discussion	137
8.5	Conclusions	140
9	Monolayer and LB films of octadecanethiol and its metal complexes	143
9.1	Introduction	143
9.2	Experimental	144
9.3	Results and Discussion	145
9.3.1	ODT molecules at air-water and air-silicon interfaces	145
9.3.2	Monolayer of ODT on alkaline subphase	154
9.3.3	Metal complexes of ODT molecules	158
9.3.3.1	Effect of divalent ions (Cd^{2+}) in the subphase	158
9.3.3.2	Effect of trivalent ions (Au^{3+}) in the subphase	162
9.4	Conclusions	166
	Appendices	169
A	Functionalized gold particles	169
B	Instrumentation for reflection absorption infrared spectroscopy: Study of tilt and ordering of the molecules in the LB films	170

Acknowledgements

I am deeply indebted to Prof. Kattera A. Suresh for his inspiring guidance and constant encouragement. I thank him for his enormous patience during the entire course of this work. I benefited immensely from his constructive criticism and suggestions. It has been a pleasure to work with him. He was also helpful in non-academic issues.

I am very much thankful to Prof. G. S. Ranganath for many useful discussions. I thank him for listening to me and giving valuable suggestions. I am thankful to Prof. Satyendra Kumar for his kind help in providing atomic force microscope facility in Kent State University.

I am extremely thankful to Prof. Sandeep Kumar for helpful discussions regarding basic chemistry and synthesizing some very useful molecules. Thanks are also due to Prof. V. Lakshminarayanan for scanning tunneling microscopy and for many fruitful discussions. I am grateful to Prof. S. Yashonath of IISc for helpful discussions on computer simulation and for providing me facility at Supercomputer Education and Research Centre in IISc. I thank Dr. V. A. Raghunathan, Prof. N. V. Madhusudana, Dr. Yashodhan Hatwalne, Dr. Abhishek Dhar and Prof. N. Udaya Shankar for many helpful discussions. I would like to thank Dr. R. Pratibha for providing IR polarizer and discussions related to the experiments.

I would like to thank Prof. N. Kumar for his interest in my work and encouragement.

I would like to thank people in the chemistry lab for providing a copious amount of distilled water for our Millipore system and for many useful solvents.

I am very thankful to Mr. M. Mani, Mr. Ram (H. Subramanyam) and Mr. A. Dhason of LC laboratory. Mr. M. Mani has very nicely machined the setup for variable temperature reflection absorption infrared spectroscopy. Mr. Ram was of great help in providing metal deposited substrates and Mr. A. Dhason in providing glasswares. I would like to express my sincere thanks to Mrs. K. N. Vasudha who helped not only as a technical staff but also as a good friend.

The library in RRI is equipped with a very good collection of books and scientific journals. I would like to express my deep gratitude to the highly efficient and extremely

helpful library staff.

I would like to thank people in the computer section for providing good computing facilities and giving larger disk quota whenever I requested.

I am very thankful to the people in the administration and accounts sections for efficiently handling my official issues. I am particularly thankful to Mr. K. Krishnama Raju and Mr. K. R. Shankar for their timely help at various occasions. I thank Mr. K. Radhakrishna, LC secretary, for his help and cooperation.

I am thankful to the canteen staff who always cheerfully provided hygienic food.

My special thanks to Viswanath for providing a cordial and friendly environment in the laboratory. His suggestions were of great use. My sincere thanks to Amit, Manjula and Surajit for their help and suggestions in academic matters. I thank Alpana and Bharat for their help in various ways.

I am extremely thankful to Sanat for his help in academic and non-academic matters. I appreciate his caring and supporting personality. My heartfelt thanks to Dipankar, Manjula and Chandrakanta for their support and encouragement during my tough time.

I would like to thank Surajit, Uday, Ujjal, Pani, Shreenivas, Amarnath, Rema, Pandey, Brindaban, Shantanu, Jayadevaiah, Karthikeyan, Srikanth and Anita. I had a wonderful time in RRI in the company of these people. My thanks to everyone at RRI for their support and cooperation in various ways which made my stay very enjoyable.

I thank my mother, Malati Gupta for her constant support and sacrifices. I have great pleasure in dedicating my thesis to my dear mother. I profusely thank my brother and sisters for their encouragement and support throughout my academic career.

List of symbols used frequently in the thesis

π	Surface pressure
π_c	Collapse pressure
π_t	Target surface pressure
A_m	Area per molecule
A_o	Limiting area per molecule
A_i	Lift-off area per molecule
A_t	Area per molecule at time t
$A_{t=0}$	Area per molecule at initial time
A_{id}	Ideal area per molecule
A_{ex}	Excess area per molecule
ΔG	Excess Gibbs free energy
E	In-plane elastic modulus
γ	Surface tension of water with monolayer
γ_o	Surface tension of water
τ	Transfer ratio
n	number of cycles of LB deposition
η_n	Effective adsorption after nth cycle
k_B	Boltzmann constant
T	Absolute temperature
t	temperature in °C
X_1	Mole fraction of component 1 in a mixture of the components 1 and 2
A	Absorbance
ν	Wavenumber
M	Transition dipole moment
N_a	Avogadro's number
L_1	Low density liquid
L'_1	Low density liquid with varying tilt-azimuth of the molecules
L_2	Low density liquid with uniformly tilted molecules
L_2	High density liquid with untilted molecules
L_{1d}	Low density disordered liquid
L_{1o}	High density ordered liquid
B_{1o}	Bilayer of L_{1o}
$R_{\alpha,\alpha'}$	Ratio of the absorbance in the phases α and α'

List of abbreviations used in the thesis

LB	Langmuir-Blodgett
SAM	Self-assembled monolayer
BAM	Brewster angle microscope
AFM	Atomic force microscope
STM	Scanning tunneling microscope
ChA	Cholesteric acid
Ch	Cholesterol
SA	Stearic Acid
DPPC	L- α -dipalmitoyl phosphatidylcholine
TCh	Thiocholesterol
TCQ	Tricycloquinazoline
AmTCQ	Amphiphilic TCQ based discotic mesogen
FGP	Functionalized gold particle
TEM	Transmission electron microscope
ODT	Octadecanethiol
ESP	Equilibrium spreading pressure
RAIRS	Reflection absorption infrared spectroscopy
HOPG	Highly oriented pyrolytic graphite
HMDS	Hexamethyldisilazane

Preface

This thesis deals with the studies on the phase transitions, stability, complex formation, and the molecular aggregations in the Langmuir monolayer and Langmuir-Blodgett films of mesogenic and organometallic amphiphilic molecules. A single layer of insoluble amphiphilic molecules spread at the air-water (A-W) interface is called a Langmuir monolayer. The Langmuir monolayer provides an ideal two-dimensional (2D) system to study the surface thermodynamics at the air-water (A-W) interface. Langmuir monolayer shows a variety of 2D phases depending on the nature of interaction among the molecules and experimental conditions, such as temperature, pH and ion contents of the subphase [1]. Some of the most commonly observed phases are; gas, low density liquid (L_1), high density liquid (L_2) and solid (S) phases. Beyond the solid phase, the monolayer exhibits the collapsed state. In the collapsed state, the molecules form multilayer or 3D crystalline flakes. It has been reported that aliphatic chain derivatives exhibit 17 different phases [2].

We have employed surface manometry to study the phase transitions in the Langmuir monolayer. In surface manometry, surface pressure (π) is varied as a function of area per molecule (inverse of surface density) at a constant temperature. The surface pressure is defined as

$$\pi = \gamma_o - \gamma$$

where γ_o and γ are the surface tensions of water without and with monolayer, respectively. Conventionally, a plateau in the isotherm indicates the coexistence of the phases and a kink represents a phase transition. We have employed Brewster angle and epifluorescence microscopes for observing the phases in the monolayer.

Langmuir monolayer can be transferred layer by layer onto a solid substrate by Langmuir-Blodgett (LB) technique [3]. Such LB films can be used in sensors, molecular electronics, non-linear optical and electrical devices [3, 4]. We have studied the LB films using atomic force microscopy, scanning tunneling microscopy and grazing angle reflection absorption infrared spectroscopy (RAIRS). The RAIRS setup was designed, fabricated and calibrated by us in our laboratory.

There are some interesting amphiphilic mesogenic molecules which assemble to yield a variety of surface phases at the A-W interface. Clusters of metallic atoms can be functionalized chemically with organic ligands to furnish it with an amphiphilic nature. We name such molecules as organometallic, that is the organic ligands to the metallic clusters. Such functionalized molecules, when spread on the water surface, yield a stable Langmuir monolayer. In chapter 1, we describe the monolayer and multilayer systems and have given the experimental details for studying them at the A-W and air-solid interfaces.

Chapter 2 deals with our studies on the Langmuir monolayer properties of a mesogenic molecule, cholesteric acid. The molecule possesses an anisotropy in size of its polar and non-polar parts. The molecule is chiral and it shows a high value of right handed specific optical rotation. It exhibits the cholesteric liquid crystal phase in a temperature range of 146.7 to 148.5°C. We find that the cholesteric acid (ChA) molecules form a stable Langmuir monolayer at the A-W interface. The surface pressure (π) - area per molecule (A_m) isotherm of the ChA monolayer at the A-W interface reveals three kinks indicating three phases (Figure 1). The regions of the isotherm **a–b**, **b–c** and **c–collapse** are designated as the L_1' , L_2' and L_2 phases. The Brewster angle microscopy of ChA monolayer at the A-W interface reveals interesting patterns. The image in the L_1' phase (Figure 2) shows a feature consisting of stripes and spirals. Immediately after compressing the monolayer to the L_1' phase, we find a few stripes and small spirals. The number of stripes and the size of the spirals grow with time. Also, the spirals rotate with time. Figure 3 shows such images for the ChA monolayer in the L_1' phase with time. Here, the two images depict the rotation of the spirals. Interestingly, we find the spirals to rotate in the right-handed direction, as indicated by the arrows in the images. The pattern relaxes eventually to an equilibrium state showing larger spirals and stripes of varying width. The stripe width varies in the range of 20 to 100 μm .

The BAM and epifluorescence observations indicate that the L_1' phase is liquid-like. The intensity modulation in the observed BAM images giving rise to stripe patterns in the L_1' phase, can be attributed to the tilt-azimuthal variation of the molecule in the monolayer. The presence of a point defect in the monolayer leads to the appearance of spirals in the BAM

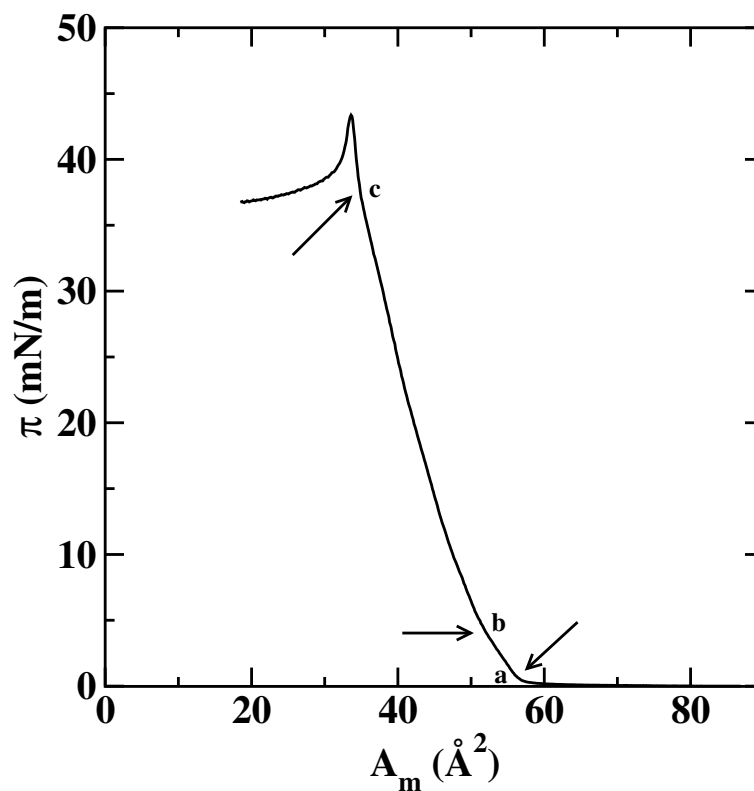


Figure 1: Surface pressure (π) - area per molecule (A_m) isotherm of cholesteric acid (ChA) monolayer on the ultrapure ion-free water. The kinks in the isotherm are indicated by the arrows. Their positions in the isotherm are shown by **a**, **b** and **c**.

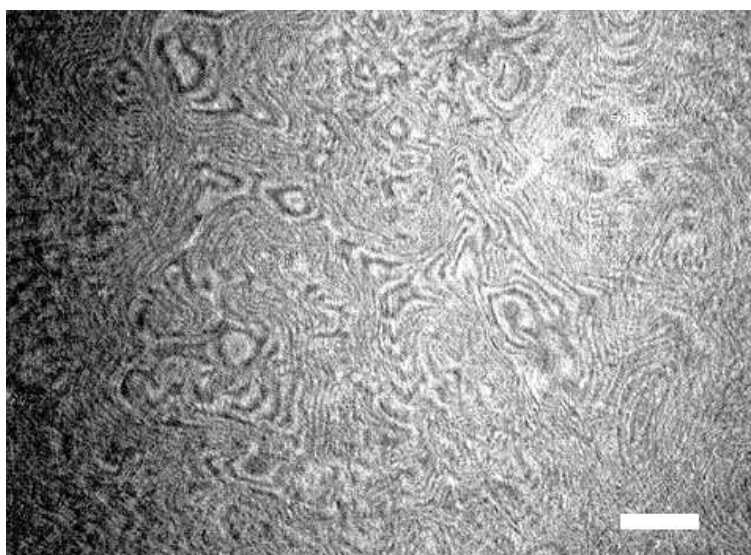


Figure 2: BAM image of the ChA monolayer on the ultrapure ion-free water captured immediately in the L'_1 phase after holding the barriers at an A_m of 54.7 \AA^2 . The image shows stripes and spirals. The scale bar represents $500 \mu\text{m}$.

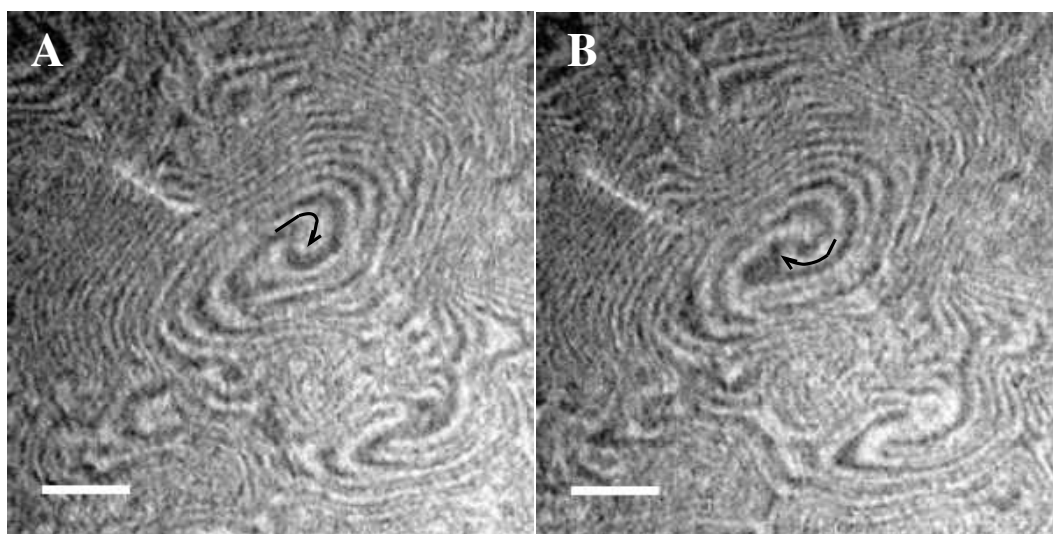


Figure 3: BAM images of the ChA monolayer on the ion-free water captured at an A_m of 54 \AA^2 after four minutes of holding the barriers. The time interval between images A and B is two seconds. The arrow on one arm of the spiral depicts its sense of rotation. The scale bar represents 335 \mu m .

images. The definite right-handed rotation of the spirals can be related to the molecular chirality. The rotation of the spirals in a monolayer was predicted theoretically by Selinger and Selinger [5]. However, this is the first experimental observation showing the rotating spirals.

The BAM images in the other phases, L'_2 and L_2 show a uniform texture. The epifluorescence microscope images of the ChA monolayer at the A-W interface reveal a uniform texture throughout the monolayer regime. The surface manometry and microscopy studies indicate that the L'_2 and L_2 phases are liquid-like with uniformly tilted molecules and a condensed phase with untilted molecules, respectively. The incorporation of metal ions in the subphase suppresses the L'_1 phase, whereas it stabilizes the L_2 phase. Metal ions added to the subphase form a complex with the ChA molecules in the monolayer at the interface leading to a condensation effect on the monolayer.

In chapter 3, we describe the studies on the stability of the phases and miscibility of binary mixture of ChA molecules and the molecules of different structures. We have chosen the lipid molecules like cholesterol (Ch), stearic acid (SA) and L- α -dipalmitoyl phosphatidylcholine (DPPC) for such studies. With a structurally similar molecule like Ch, ChA molecules show a miscible behavior for all the compositions and at all surface

pressures. For the mole fraction of Ch in ChA (X_{Ch}) greater than 0.5, the L'_1 phase gets suppressed and the mixed monolayer exhibits only L'_2 and L_2 phases. The variation of excess Gibbs free energy (ΔG) as a function of X_{Ch} indicates that the most stable composition is 0.7 mole fraction of Ch in ChA. The variation of excess area per molecule (A_{ex}) with respect to X_{Ch} indicates an attractive interaction between the Ch and ChA molecules in the mixed monolayer. Based on our studies, we have constructed a phase diagram of the mixed monolayer of Ch and ChA molecules.

The studies on the mixed monolayer system of ChA and a linear molecule like stearic acid (SA) suggest a partial miscibility of the molecules. The variation of ΔG as a function of mole fraction of SA in ChA (X_{SA}) indicates that the stable composition is around 0.4 mole fraction of SA in ChA. The other compositions were found to be unstable.

The bulkier molecule, such as DPPC mixes readily in the ChA monolayer. The presence of DPPC in the ChA monolayer suppresses the L'_1 phase, whereas it stabilizes the L_2 phase. The variation of ΔG with mole fraction of DPPC in ChA (X_{PC}) indicates that the mixed monolayer is stable, and the most stable composition is 0.5 mole fraction of DPPC in ChA.

Chapter 4 deals with the studies on the mixed monolayer of Ch and thiocholesterol (TCh). The TCh molecule differs from the Ch molecule only in the replacement of -OH group by -SH group at its 3β position. Though the Ch molecules form a stable monolayer at the A-W interface exhibiting gas, untilted condensed (L_2) phase and a collapsed state, TCh molecules do not form a monolayer at the interface. However, the presence of TCh molecules in the Ch monolayer at the A-W interface changes the nature of the isotherm (Figure 4). The isotherm shows an additional change in the slope which can be considered as an initial collapse of the two component monolayer system. The surface manometry and the microscopy observations suggest that the mixed monolayer exhibits the untilted condensed (L_2) phase in the region corresponding to the steep rise in surface pressure. Above the initial collapse, the TCh molecules squeeze out from the mixed monolayer. Also, there is a final collapse of the mixed monolayer system. The initial collapse represents the collapse of the mixed monolayer, whereas the final one represents the collapse of the Ch rich monolayer. The variation of the

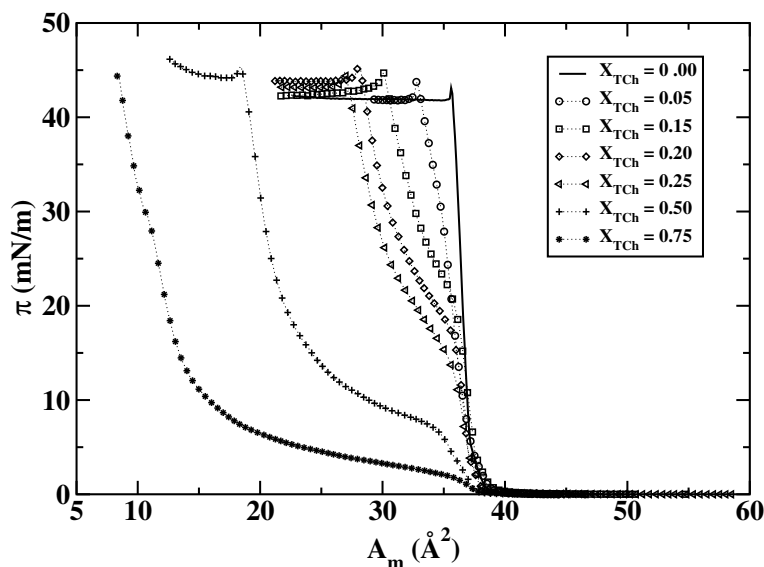


Figure 4: The surface pressure (π) - area per molecule (A_m) isotherms of the mixed monolayer for different mole fractions of TCh in Ch (X_{TCh}).

A_{ex} as a function of mole fraction of TCh in Ch indicates an attractive interaction between the Ch and TCh molecules.

In chapter 5, we present our AFM studies on LB films of Ch deposited on hydrophobic substrates at a target surface pressure (30 mN/m) corresponding to the untilted condensed (L_2) phase. Ch molecule is largely hydrophobic in nature. Hence, the interaction between the hydrophilic substrates and the Ch molecules are weak to support the multilayer formation during the LB deposition. On the other hand, the Ch molecules exhibit much better adhesion on hexamethyldisilazane (HMDS) treated hydrophobic glass substrates. During each cycle of LB deposition, it was clear from the transfer ratio data that downstrokes adsorb the molecules efficiently while the upstrokes desorb fraction of the earlier deposited layers. Beyond four cycles of deposition, there was no effective adsorption. The AFM imaging of the different cycles of deposited films yields interesting patterns. The AFM image for one cycle of deposition shows a uniform film of Ch molecules oriented normal to the substrate. For the two cycles of deposition, the image (Figure 5(a)) shows elongated domains of normally oriented molecules on the top of another uniformly covered monolayer. Interesting features were seen in the image for four cycles of deposited film (Figures 5(b) and 6(a)). It reveals a uniformly distributed torus-shaped domains (doughnuts) having an average outer diameter

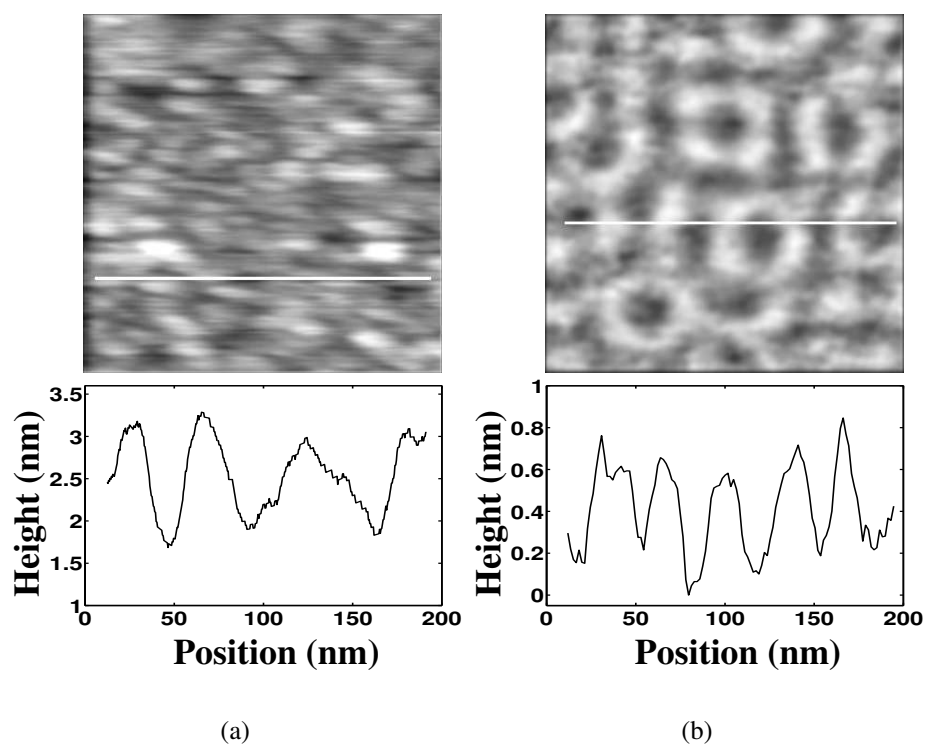


Figure 5: (a) and (b) represent the LB films of cholesterol (Ch) molecules on the hydrophobic substrate deposited during two and four cycles, respectively. The white line on the images is drawn to measure the height variation along it. The corresponding height profiles are shown below the respective images. The image size in each case is $200 \times 200 \text{ nm}^2$.

of about 65 nm and annular width of about 22 nm. The analysis suggests that the height variation in the torus-shaped domains is due to the tilting of the Ch molecules in the film. The phase image of the four cycles of deposited film shows that the doughnuts are asymmetric and only one side gives dark and bright regions (Figure 6(b)). The bright regions in the phase image correspond to the polar regions of the LB film [6]. This indicates the projection of -OH group of the Ch molecules to be away from the substrate. However, for the dark regions in the phase images, we suggest that it corresponds to less polar regions of the LB film. The less polar regions may be due to flipping of the Ch molecules in the LB film, as reported in literature [7]. Hence, the four cycles of deposition yields a layer of gradually tilting molecules and some region of flipped molecules on the top of another uniformly deposited layer. The formation of the torus-shaped domains in the LB films of Ch are due to the reorganization of the molecules on the hydrophobic substrate during adsorption and

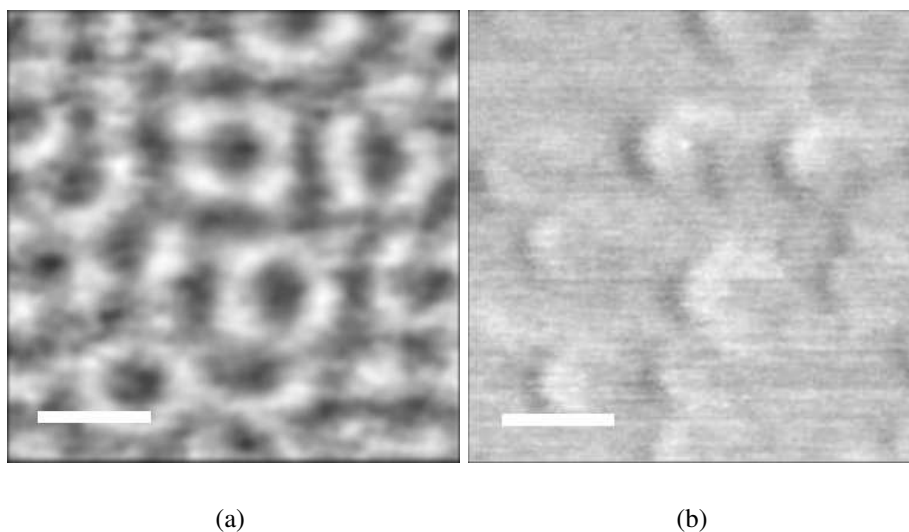


Figure 6: (a) and (b) represent the height and the phase images of the the four cycles of deposition of Ch, respectively. The scale bar represents 50 nm.

desorption. This is the first report presenting the interesting molecular assemblies due to the adsorption and desorption of the molecules during LB deposition.

In chapter 6, we describe scanning tunneling microscope and computer simulation studies on the orientation and ordering of Ch molecules in the LB film deposited on graphite substrate. We have transferred one layer of LB film of Ch at a target surface pressure of 3 mN/m on a highly oriented pyrolytic graphite (HOPG) substrate. The STM image of the HOPG substrate reveals a corrugation of 0.24 nm which indicates the lateral separation of the β atoms in a graphene plane [8]. The STM image of the LB film of Ch on HOPG shows a highly periodic texture of wire-network (Figure 7). The intensity profile data reveal the distance between the two bright regions separated by a dark region to be 0.5 nm. Such an ordered texture reveals a two-dimensional oblique lattice. We find the magnitude of the lattice parameters \mathbf{a} and \mathbf{b} to be 0.705 and 0.727 nm, respectively. The angle between them was found to be 39.8° . To interpret such STM images, we have undertaken computer simulation studies. Here, we place the Ch molecules on the graphite [0001] plane, and the conformation of the molecules were monitored as a function of surface density. For any particular value of the surface density, 10 different random initial conformations of

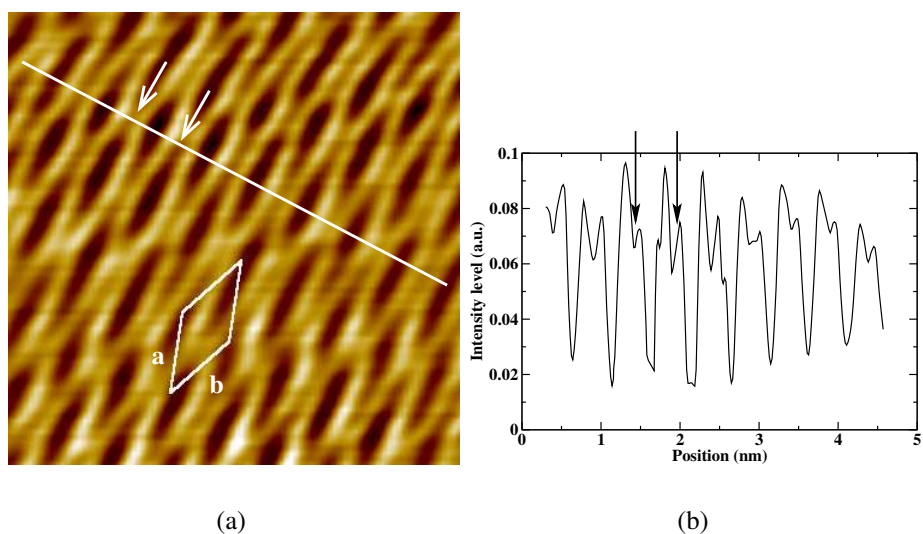


Figure 7: (a) shows the STM image of the LB film of cholesterol on HOPG. The image was taken in constant height mode at 100 mV bias voltage and 1 nA tunneling current. (b) shows the intensity profile along the white straight line drawn on (a). Arrows are drawn to show the corresponding positions in the image and the graph. The distance between the two arrows is 0.5 nm. An oblique rectangular shape is drawn in (a) to represent a single 2D lattice cell. Here, **a** and **b** represent the lattice parameters. The size of the image in (a) is $4 \times 4 \text{ nm}^2$.

the Ch molecules were chosen, and the energy of the system was minimized for each individual initial conformation. The final conformation of the molecules was chosen such that it represents the system of the lowest energy among the 10 different initial conditions. The tilt angle (θ) of the molecule is defined as the angle between the long molecular axis and the substrate normal (Z-axis). We have determined the θ values from the minimized conformations at various surface densities on the substrate. A histogram showing the distribution of θ is presented in Figure 8. The distribution of θ shows a peak at around 89° . This indicates a planar orientation of the Ch molecule on the [0001] plane of the graphite substrate. The Ch can be considered as an electron deficient molecule. However, the substrate, HOPG is very rich in electron and is atomically smooth. We expect that the bright region in the STM images are mainly due to the overlapped molecular orbitals of the graphite and the cholesterol. The dark region can be assigned to the electron deficient core of the cholesterol molecule. We suggest a possible arrangement of the molecules in the LB film on the HOPG substrate, as depicted in Figure 9. In the previous chapter, we find that

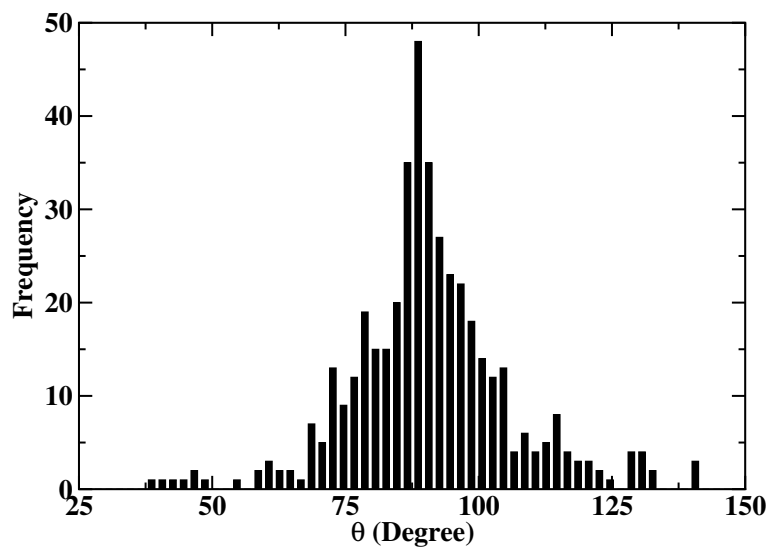


Figure 8: Histogram showing the distribution of the tilt angle (θ) of the cholesterol molecules with respect to the substrate normal. Here, the sample points are 434 and the bin size is 2° .

the Ch molecules adsorb efficiently on a hydrophobic substrate as compared to a hydrophilic substrate. The LB film of Ch on a hydrophobic HOPG substrate was deposited in the phase corresponding to the untilted condensed (L_2) phase. Surprisingly, the transfer ratio was very small (0.2 to 0.3). This indicates that unlike the case of Ch on hydrophobically treated glass

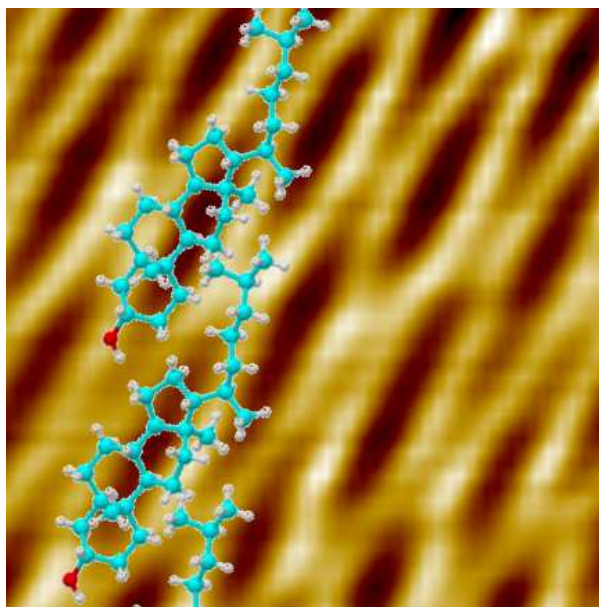
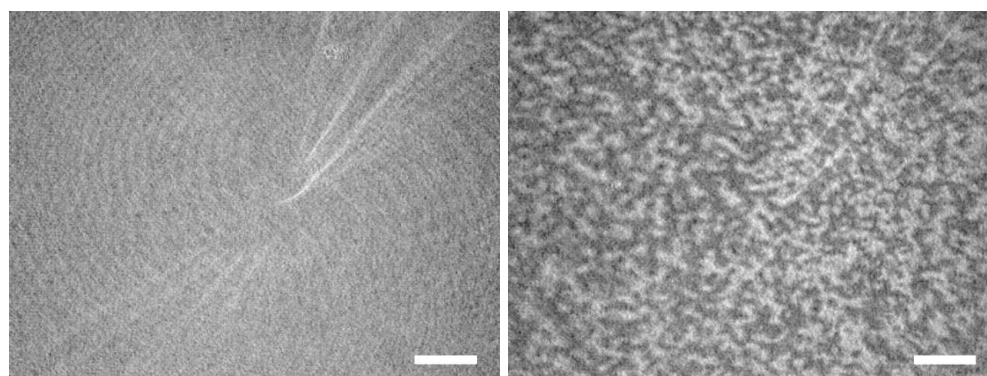


Figure 9: A $2.38 \times 2.38 \text{ nm}^2$ STM image of the LB film of the cholesterol molecules on HOPG substrate. Here, the cholesterol molecules are shown to depict a possible conformation of the molecules on the substrate.

substrate, the normal orientation of the Ch on HOPG substrate is not favored. We suggest that the cholesterol molecules after being transferred from A-W interface to the graphite substrate, rearrange themselves with a planar orientation. Such a rearrangement yields an ordered assembly of Ch molecules as observed using STM.

Discotic liquid crystals, which were discovered in 1977 [9], have drawn lot of attention. The assembly and aggregation of such molecules on surfaces are of considerable interest. Chapter 7 deals with studies on Langmuir monolayer and LB film of discotic mesogenic molecules. The molecule possesses tricycloquinazoline (TCQ) core and six polar ethylenoxy side-chains which are symmetrically attached to the TCQ core so that it retains its C_3 fold symmetry. We denote this molecule by the symbol AmTCQ. We find that the AmTCQ molecules yield a stable Langmuir monolayer. In the monolayer, a disk-like molecule may align with its core parallel (face-on) or perpendicular (edge-on) to the interface. The surface manometry and Brewster angle microscopy suggest a face-on conformation of the molecules at large A_m . Interestingly, in the A_m range of 180 to 100 \AA^2 (steep region of the isotherm), the monolayer exhibits a coexistence of both the face-on and edge-on molecular conformations. The BAM image of the AmTCQ monolayer at the A-W interface reveals an uniform gray texture at a very large A_m (Figure 10(a)). The image in the steep region of the isotherm (Figure 10(b)) shows the bright domains in the gray background. The intensity in the BAM images depends on the thickness of the film and the orientation of the molecules [10]. From our surface manometry and microscopy studies, we show that the bright domains in the image corresponds to the domains of the molecules with edge-on conformation and the gray background represents a face-on conformation. This is the first observation where a system of discotic monolayer at the A-W interface exhibits a stable phase of the coexistence of both the molecular conformations.

In chapter 8, we describe our studies on the monolayer of functionalized gold particles (FGP). The cluster of gold atoms was chemically attached to monolayer of organic ligands such as mercapto-1-undecanol and hexanethiol. The ligand mercapto-1-undecanol has terminal -OH group which renders an amphiphilic nature to the particle. We refer to



(a) $A_m = 250 \text{ \AA}^2$

(b) $A_m = 125 \text{ \AA}^2$

Figure 10: BAM images of the AmTCQ monolayer on the ion-free water. The images were captured at an A_m shown below the respective images. (a) shows a uniform gray texture representing a face-on conformation of the molecules. (b) shows a coexistence of bright domains in the gray background. The bright region corresponds to the domains of AmTCQ with edge-on molecular conformation. The scale bar represents $500 \mu\text{m}$.

such particles as organometallic. This molecule is synthesized in our Institute [11]. The transmission electron microscope (TEM) image yields an average diameter of the core to be 5.5 nm (Figure 11). Assuming the organic ligands to be uniformly covering the gold particle, the diameter of the FGP for the fully stretched ligands was estimated to be 8.4 nm . Therefore, the cross-sectional area of each particle will be 55.4 nm^2 . The surface pressure - area per molecule isotherms were obtained at different temperatures. The isotherms at low

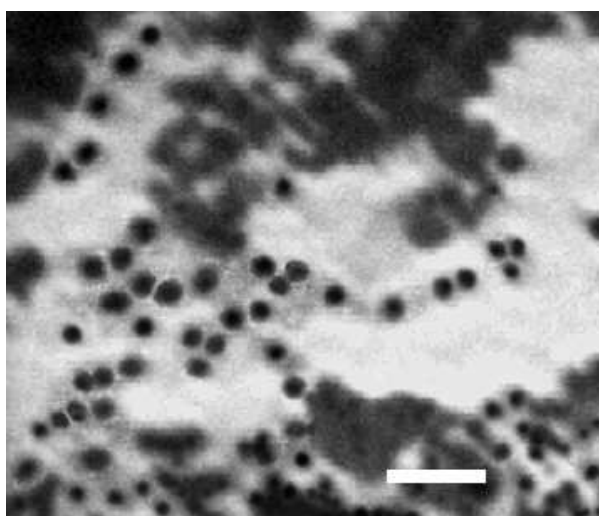


Figure 11: The transmission electron microscope image of the FGP. The black circles represent the core of the FGP. It has a mean diameter of 5.5 nm . The scale bar represents 25 nm .

temperature ($<28\text{ }^{\circ}\text{C}$) show a slow rise in surface pressure followed by a small plateau and a steep rise in surface pressure. The average area occupied by a molecule in a phase can be determined by extrapolating the corresponding region of the isotherm to the zero surface pressure. The average area occupied by FGP in steep region of the isotherm was 61 nm^2 . This is in good agreement with the size of particles determined from TEM images. The phases corresponding to the slow rise and steep rise in surface pressure in the isotherm, were denoted as the L_{1d} and L_{1o} phases, respectively. We find a first order transition from L_{1d} to L_{1o} phase. We have estimated the value of critical temperature (t_c) to be $28.4\text{ }^{\circ}\text{C}$. In the temperature range of 29 to $36\text{ }^{\circ}\text{C}$, the monolayer exhibits the L_{1d} and B_{1o} phases. The results of surface manometry indicate B_{1o} to be a bilayer of L_{1o} phase. We have observed the monolayer of FGP using BAM at different temperatures. The results of BAM imaging are consistent with those obtained from the surface manometry. We have transferred the LB films of FGP at different target surface pressures (π_c) corresponding to the different phases. The LB films were analyzed by RAIRS. The spectra are shown in Figure 12. The analysis of the spectra indicates that the L_{1o} phase is denser than L_{1d} phase and B_{1o} phase is a bilayer of the L_{1o} phase. The results of the RAIRS are in agreement with that of surface manometry results.

The surface manometry, Brewster angle microscopy and RAIRS indicate that the system exhibits a low density disordered liquid (L_{1d}), high density ordered liquid (L_{1o}) and bilayer of L_{1o} (B_{1o}) phases. Based on these studies, we present a phase diagram shown in Figure 13.

This is the first report on such a novel molecule which exhibits interesting phases in a Langmuir monolayer.

Chapter 9 deals with the studies on the Langmuir monolayer and LB films of the octadecanethiol (ODT) molecules and its metal-complexes. Our studies reveal that ODT forms a very stable Langmuir monolayer at the A-W interface provided the subphase is ultrapure ion-free water with a resistivity greater than $18\text{ M}\Omega\text{-cm}$. However, we find that the monolayer is very sensitive to the presence of very small quantities of NaOH or the salts (CdCl_2 and $\text{AuCl}_3\cdot\text{HCl}$) in the aqueous subphase. The AFM image of the LB film

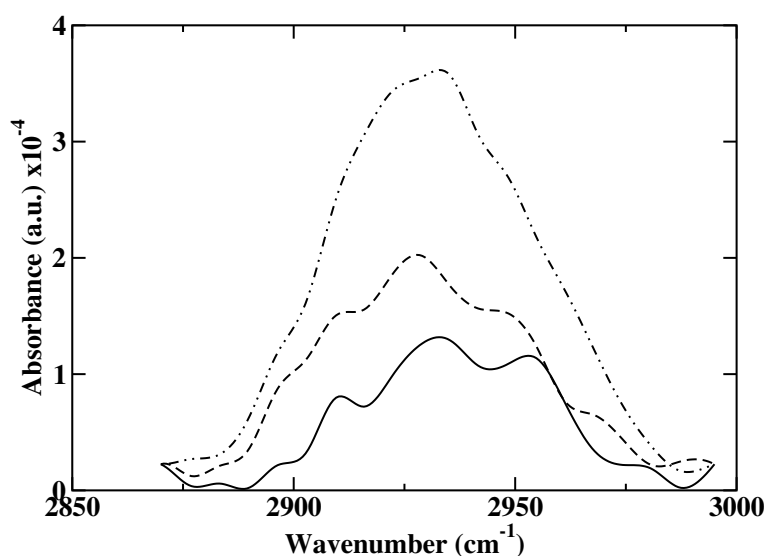


Figure 12: Reflection absorption infrared spectra for the LB films of FGP on gold substrate deposited at the different target surface pressures corresponding to different phases. The vibration band represents the stretching mode of the alkyl chains (CH) of FGP. The solid (—) and the dashed (---) lines represent the spectra for the LB films transferred at a temperature of 25.0 °C and at the surface pressures of 4 and 20 mN/m, respectively. The spectra correspond to the L_{1d} and L_{1o} phases, respectively. The dotted-dashed line ($\cdot\cdot\cdot$) represents the spectrum of the LB film transferred at a temperature of 31.0 °C and at a surface pressure of 27 mN/m. The spectrum corresponds to the B_{1o} phase.

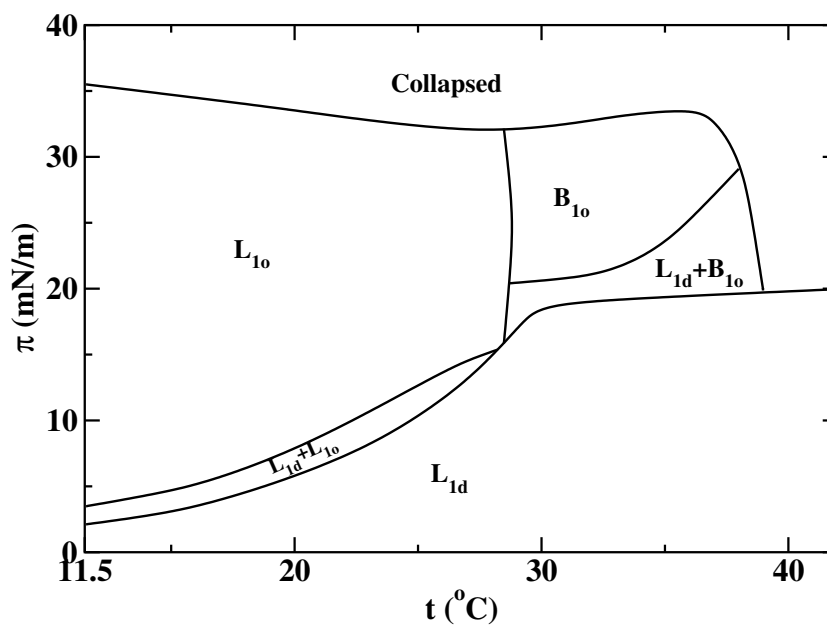


Figure 13: Phase diagram showing the monolayer phases of the functionalized gold particles. Here, t represents the temperature of the subphase and π represents the surface pressure. The symbols L_{1d} , L_{1o} and B_{1o} represent low density disordered liquid, high density ordered liquid and bilayer of L_{1o} phases, respectively. The L_{1d} and gas phase coexistence was seen even at very large A_m and zero surface pressure.

of ODT molecules deposited from ion-free water on the silicon (Si) substrate is shown in Figure 14. It shows streak-like bright domains grown on the uniform gray background. The

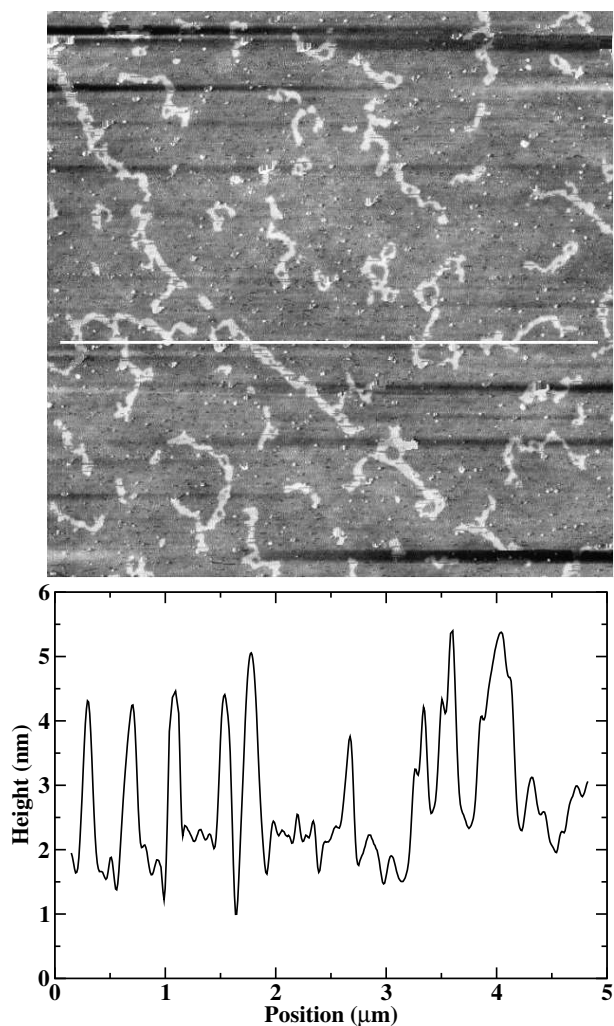


Figure 14: AFM image of the LB film of ODT molecules deposited from ion-free water on a silicon substrate. The white line in the image represents the line along which the height profile is drawn. The height profile is shown below the image. The size of the image is $5 \times 5 \mu\text{m}^2$.

image also shows bright and dark spots embedded all over the gray background. We find that the average height of the gray background is 2 nm and that of the streak-like domains and the bright spots are 4.3 nm. The length of an ODT molecule is 2.1 nm. Hence, the gray background represents a layer of ODT molecules oriented normal to the Si substrate. The streak-like domains represent the bilayer of normally oriented molecules and the dark spots are the defects in the film.

The ODT monolayer behaves differently with divalent and trivalent ions in the subphase.

The presence of divalent ion (Cd^{2+}) in the subphase reveals the formation of bilayer at the A-W interface. The AFM images of the LB film of the ODT molecules deposited from a subphase containing the very low concentration of CdCl_2 show the dendritic domains. The dendritic domains represent a layer of the complex unit. A crystalline monolayer was observed due to the presence of trivalent ion (Au^{3+}) in the subphase. Here, the BAM images showed an uniform crystalline film. The AFM images of the LB film of ODT molecules deposited from a subphase containing very low concentration of $\text{AuCl}_3 \cdot \text{HCl}$ revealed the monomolecular thick domains of ODT molecules oriented normal to the substrate and thick domains of the complex of ODT and $\text{AuCl}_3 \cdot \text{HCl}$.

The papers describing some of these works have been sent for publication. Other manuscripts are under preparation.

1. AFM studies on Langmuir-Blodgett films of cholesterol, *Raj Kumar Gupta and K. A. Suresh*, Euro. Phys. J. E **014**, 35 (2004).
2. Stability of the Langmuir monolayer of octadecanethiol, *Raj Kumar Gupta and K. A. Suresh*, (Communicated)

Bibliography

- [1] G. L. Gaines, Jr., *Insoluble Monolayers at Liquid-Gas Interfaces* (Wiley-Interscience, New York, 1966).
- [2] V. M. Kaganer, H. Möhwald, and P. Dutta, *Rev. Mod. Phys.* **71**, 779 (1999).
- [3] G. Roberts (Editor), *Langmuir-Blodgett Films* (Plenum, New York, 1990).
- [4] A. Ulman, *An Introduction to Ultrathin Organic Films From Langmuir-Blodgett to Self-Assembly* (Academy Press Inc., San Diego, 1991).
- [5] J. V. Selinger and R. L. B. Selinger, *Phys. Rev. E* **51**, R860 (1995).
- [6] D. Raghavan, X. Gu, T. Nguyen, M. VanLandingham, and A. Karim, *Macromolecules* **33**, 2573 (2000).
- [7] D. Y. Takamoto, E. Aydil, J. A. Zasadzinski, A. T. Ivanova, D. K. Schwartz, T. Yang, and P. S. Cremer, *Science* **293**, 1292 (2001).
- [8] S. Hembacher, F. J. Giessibl, J. Mannhart, and C. F. Quate, *Proc. Natl. Acad. Sci. U. S. A.* **100**, 12539 (2003).
- [9] S. Chandrasekhar, B. K. Sadashiva, and K. A. Suresh, *Pramana* **9**, 471 (1977).
- [10] S. Rivière, S. Hénon, J. Meunier, D. K. Schwartz, M.-W. Tsao, and C. M. Knobler, *J. Chem. Phys.* **101**, 10045 (1994)
- [11] Sandeep Kumar, (To be published)